An Experimental Investigation on the Material Removal Rate and Surface Roughness of a Hybrid Aluminum Metal Matrix Composite (Al6061/SiC/Gr)

Mandeep Singh [1],*, Harish Kumar Garg [2], Sthitapragyan Maharana [1], Anchal Yadav [3], Rasmeet Singh [4], Pragyansu Maharana [1], Tien V. T. Nguyen [5], Sudesh Yadav [6] and M. K. Loganathan [7]

1   School of Mechanical and Mechatronic Engineering, University of Technology Sydney, Sydney, NSW 2007, Australia; sthitapragyan.maharana@student.uts.edu.au (S.M.); pragyansu.maharana@student.uts.edu.au (P.M.)
2   Department of Mechanical Engineering, D.A.V. University Jalandhar, Jalandhar 144001, India; harish10026@davuniversity.org
3   School of Chemistry, Monash University, Clayton, VIC 3168, Australia; anchal.yadav@monash.edu
4   Dr. S.S. Bhatnagar University Institute of Chemical Engineering & Technology, Panjab University, Chandigarh 160014, India; srasmeet9@gmail.com
5   Industrial University of Ho Chi Minh City, Ho Chi Minh City 70000, Vietnam; thanhtienck@naver.com
6   Centre for Green Technology, School of Civil and Environmental Engineering, University of Technology Sydney, Sydney, NSW 2007, Australia; Sudesh.Yadav@student.uts.edu.au
7   Department of Mechanical Engineering, The Assam Kaziranga University, Assam 785006, India; loganathanmk123@gmail.com
*   Correspondence: Mandeep.singh@uts.edu.au; Tel.: +61-42-038-0700

Abstract: The objective of this paper was to determine the optimum process parameters of an electric discharge machine while machining a new hybrid aluminum metal matrix composite. In this study, a new hybrid aluminum metal matrix composite was prepared, with silicon carbide and graphite particles used as reinforcements, with the help of the stir casting method. The selected electric discharge machining parameters in this study were peak current (I), voltage (V), pulse-on time (T_{on}), and tool material, while the response parameters were material removal rate and surface roughness. To machine the fabricated samples, two different types of tool materials (copper and brass) were used as electric discharge machine electrodes, and each had a diameter (Ø) of 12.0 mm. The optimal settings of the electric discharge machining parameters were determined through experiments planned, conducted, and analyzed using the Taguchi (L_{18}) technique. An analysis of variance and confirmatory tests were used to check the contribution of each machining parameter. It was found that the material removal rate increased with the increase in pulse-on time and pulse current, whereas the material removal rate decreased with the increase in voltage. On the other hand, reduced surface roughness could only be achieved when current, voltage, and pulse duration were low. It was also found that the selected electric discharge machining electrodes had a significant effect on both the material removal rate and the surface roughness.

Keywords: aluminum metal matrix composite; electric discharge machining; material removal rate; surface roughness

1. Introduction

Metal matrix composites (MMCs) are always in high demand due to their properties, which are distinctive from those of conventional materials [1,2]. Some of the features that distinguish MMCs from other, similar materials in the same category are high-temperature strength, low density, specific strength, higher thermal resistance, and a higher strength-to-weight ratio [1]. Other important properties include high fatigue, wear, and creep resistances [2]. These properties make MMCs a viable alternative to cast iron, which is

mostly used in the construction of engines and brakes in the automobile industry [2,3]. In most previous studies, the metals that have been used for metal matrix composites are aluminum and titanium [3,4]. Super alloys and copper alloys can also be used to develop MMCs [5,6]. The most widely used type of MMC is the aluminum matrix composite (AMC) [7]. One of the main reasons for the greater use of aluminum matrix composites is that they have comparatively lower cost requirements than other MMCs [7,8]. In addition, they provide excellent performance in all of the aforementioned properties of MMCs. Therefore, the scope of AMCs for new applications is increasing.

Hybrid metal matrix composites are those materials that are made up of at least two different materials and their combination provides superior properties, as compared to their individual constituents [8,9]. In hybrid metal matrix composites, different nominated materials work together to provide unique sets of properties [10]. One of the main reasons to use hybrid metal matrix composites in the automotive industry is their low weight, high stiffness, and strength [11]. However, the combination of the reinforcement and matrix can be improved as per the requirement of industries [11,12]. The manufacturing of a hybrid MMC material depends on its phases, i.e., the matrix phase and the reinforced (dispersion) phase [12]. The matrix phase is the primary phase, which has a continuous character, resulting in a ductile and less hard phase [12,13]. Generally, the matrix phase supports the dispersed phase and shares a sustainable amount of load with it [13]. On the other hand, the dispersed phase is embedded in the matrix in a discontinuous form. Normally, the dispersed phase is stronger than the matrix phase [13,14].

In this research, a new hybrid aluminum metal matrix composite was fabricated by using one of the best and most economical casting/fabrication processes, known as the stir casting method. To fabricate the new, advanced hybrid AMC material, aluminum 6061 (Al6061) was used as the matrix phase, while silicon carbide (SiC) and graphite (Gr) particles were used as reinforcements. In most previous studies [15–18], the development of aluminum metal matrix composites was mainly performed by adding only a single reinforcement in the stir casting process. No sufficient research has been conducted where both Gr and Sic hard ceramic materials are used as reinforcements to fabricate a new hybrid aluminum metal matrix composite using Al6061 as the base material. Normally, composite materials are difficult to machine via the conventional machining processes or conventional machine tools [19,20]. This is due to their greater hardness and brittleness, and perhaps also their shape, which is difficult to produce via any of the traditional methods. Most of the mechanical industries demand a superior finish, close tolerances, high production rates, and complex shapes, which are not possible to achieve using conventional manufacturing methods. Therefore, the electrical discharge machining (EDM) process has become a feasible method to machine the new hybrid metal matrix composites [21,22]. Most previous researchers [23–25] have experimented with AMCs and traditional MMCs coupled with EDM to achieve a high material removal rate (MRR) and low surface roughness (SR). Recently, the authors of [26–28] experimented with Al7075-based composite materials in EDM. They demonstrated that in the aluminum-based composite materials, different ceramic reinforcements had noteworthy effects on machining. Moreover, this study presented an investigation of the effects of EDM parameters on a newly fabricated Al6061-based hybrid aluminum composite, reinforced with hard ceramic materials.

Generally, most of the metals are considered as homogeneous, whereas composites are inhomogeneous, due to the inclusion of other materials [29]. These additions, which have properties that differ from those of the base metal, change the machining behavior of the composite. Therefore, to investigate the machinability of such metal composites, it is essential to study the nature of the reinforcements. Therefore, in this study, the EDM was performed on a newly developed hybrid composite (Al6061/SiC/Gr), and both the MRR and the SR were studied to optimize the quality of the developed composite. All the experimental plans were devised by using the Taguchi design (L_{18}) approach in Minitab software. The EDM parameters considered in this work were peak current (I), voltage (V), pulse-on time (T_{on}), and tool material (EDM electrodes). An analysis of variance

(ANOVA) technique was used to check the contribution of selected EDM machining parameters. Silicon carbide always enhances the hardness of a composite material, whereas graphite improves the self-lubricating power of a composite material [29,30]. Therefore, the machinability of a composite material is different from that of the other metals. Therefore, this study will directly help to resolve all the influencing factors that can cause variations in the final results of the machining of a composite material.

2. Materials and Methods

2.1. Materials

Aluminum hybrid metal matrix composites are an exceptional class of advanced engineered materials [31]. In this study, to develop the new hybrid aluminum metal matrix composite, both selected reinforcement materials were mixed in the base material (Al6061) in a 12% (SiC) and 5% (Gr) wt% ratio, respectively. Both SiC and Gr particles of a 200-mesh size (avg. size 75 μm) were used. To fabricate the hybrid aluminum metal matrix composite, the stir casting method was used, due to its simplicity and relatively cheap developing cost [32,33]. All the reinforcements were preheated at 650 °C for a sufficient time, before being mixed with molten aluminum, in order to prevent the formation of unwanted brittle-phase Al_4C_3.

In order to confirm the improved strengthening behavior of the developed hybrid aluminum metal matrix composite (Al6061/SiC/Gr), both the mechanical and tribological properties were investigated first. For a greater understanding, the mechanical and wear behaviors of Al6061/SiC/Gr (addition of both SiC (12%) and Gr (5%) particles), Al6061/SiC (addition of only SiC (10%) particles), and pure Al6061 were measured and compared. Table 1 shows the calculated mechanical properties of Al6061/SiC/Gr, Al6061/SiC, and Al6061. The results shown in Table 1 indicate that the yield and tensile strengths of Al6061/SiC/Gr are greater than those of Al6061/SiC and pure Al6061. The superior yield strength of Al6061/SiC/Gr has recognized the high load transfer effect. Simultaneously, ball-on-flat sliding tests were also performed to check the wear performance of Al6061/SiC/Gr, Al6061/SiC, and Al6061. The addition of reinforcement particles reduced the wear rate, as shown in Table 2.

Table 1. Comparison of mechanical properties.

Material	Elastic Modulus (GPa)	Ultimate Tensile Strength (MPa)	Yield Strength (MPa)	Hardness (H_v)
Al6061	71.2	142.2	92.1	59.8
Al6061/SiC	110	178.1	139.4	92.5
Al6061/SiC/Gr	119.2	192.8	152.7	101.7

Table 2. Wear rate comparison.

Material	Al6061	Al6061/SiC	Al6061/SiC/Gr
Wear rate (mm^3/Nm)	6.84×10^{-3}	5.21×10^{-3}	4.34×10^{-3}

Here, it can be seen that the hardness of Al6061/SiC/Gr increased by 40% compared to the base Al6061 hardness value. Moreover, all the high-performance mechanical and wear properties of Al6061/SiC/Gr make it a suitable material to use in an automobile disk braking system. Finally, all these results demonstrated the effectiveness of Al6061/SiC/Gr, which makes it an ideal material for further investigation.

In this study, all the experiments were performed on an Oscar Max Die-Sinking EDM machine (Oscar Max, Taiwan made)), as shown in Figure 1. Commercial grade EDM oil (density = 0.75 Kg/m^3) was used as the dielectric fluid during the EDM. Copper (Cu)

and brass (Br) electrodes, each of 12.0 mm diameter (∅), were used as machine electrodes. Figure 2 shows the fabricated samples and the tool electrodes. The straight polarity of electrodes was used during all the experimental work. Tool material, current (I), voltage (V) and pulse on time (T_{on}) were selected as the EDM process parameters. The selection of these EDM process parameters was completed on the basis of earlier findings in the literature and the recommendations of our previous research [34]. Further, to select the most significant levels of the designated process parameters, a pilot study was carried out, where the effects of different levels of the process parameters on the output parameters (MRR and SR) were individually investigated. Based on the results of the pilot experiments, the resulting set of parameters with certain values were selected for the design of the final experiments. The final selected EDM process parameters and their levels are shown in Table 3 below. The SEM (JSM-IT800, Japan made) images of the fabricated samples before the machining at different magnification levels are shown in Figure 3.
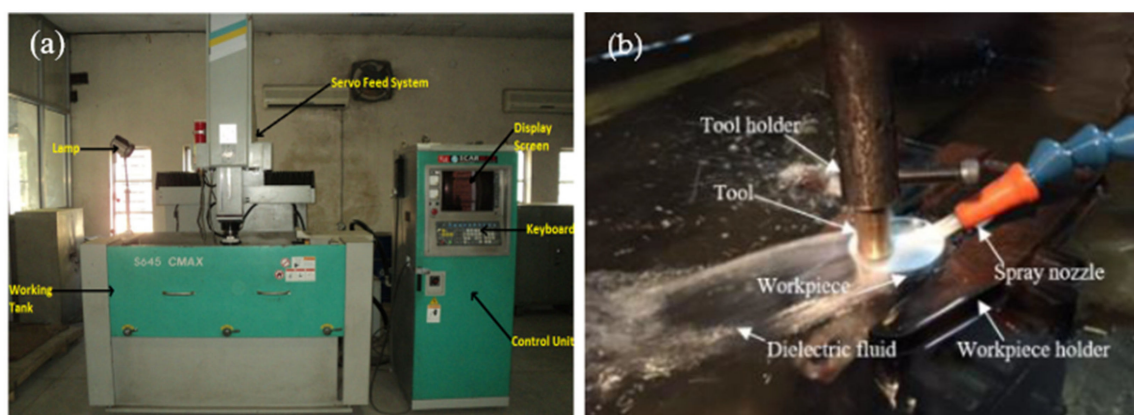

Figure 1. (**a**) EDM used for experimentation and (**b**) EDM machining.

Figure 2. Pictorial views of samples and electrodes.

Table 3. Selected EDM process parameters and their levels.

Parameters	Units	Level-1	Level-2	Level-3
Tool	-	Cu	Br	
Current (I)	Amp	10	12	14
Pulse-on time (T_{on})	μs	120	200	300
Voltage (V)	V	4	8	12

2.2. Methodology

To examine the effects of the selected EDM machining parameters, two response variables (MRR and SR) were studied. The MRR was calculated by determining the weight difference of the workpiece before and after the machining by using a digital weighing machine with 0.001 gm precision. Here, the machining time was measured by a stopwatch. A hole cavity of 1 mm depth was created during each machining process.

The surface roughness is an important element of the machined surface and here it was calculated via the vertical deviations of a machined surface from an un-machined surface. Generally, if the calculated deviation is high, then the surface is rough, and if low, then the surface is smooth. In this work, to enumerate the arithmetical mean roughness value (Ra) of the machined surface, a precise surface roughness tester (TR110Plus) was used. The travelling length of the machine was 5 mm and its measuring range was between 0.1 μm and 10.0 μm.
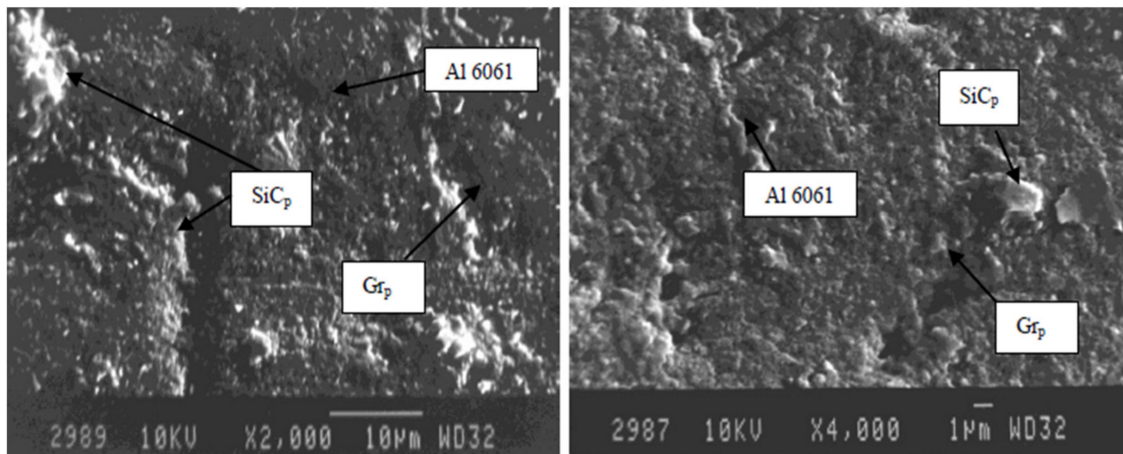
Figure 3. SEM images of Al6061/SiC/Gr before machining at different magnification levels.

Taguchi's experimental design approach always helps researchers to identify and scrutinize the prominent parameters of their research. The superior optimization performance [35] of the Taguchi approach makes it a viable optimization method. Therefore, to achieve accuracy in the output responses, the Taguchi orthogonal array $L_{18}^{(2\wedge13\wedge3)}$ was employed to design the final experiments, after the careful review of all the other optimization techniques. This selection was dependent upon a number of factors and interactions of interest, and the levels of the process parameters. Using the Minitab 14 software, the analysis of variance (ANOVA) approach was used to investigate the most significant process parameters that affect the selected response variables. The S/N ratios were calculated to identify the major contributing factors that cause variation in the MRR and SR. The S/N ratio (SNRA) was calculated by using the following formula (Equation (1)) [36]:

$$(S/N)_{HB} = -10 \log (MSD_{HB}) \tag{1}$$

where $MSD_{HB} = \frac{1}{r} \sum_{j=1}^{r} \left(\frac{1}{y_j^2} \right)$, the MSD_{HB} stands for mean square deviation for the higher-the-better response, 'r' is the number of trials, and 'y_j' is the value of the MRR for the jth test.

3. Results and Discussion

This study was highly focused on obtaining optimum levels of the MRR and SR. Therefore, higher-the-better and smaller-the-better characteristics were employed for the MRR and SR, respectively. The changes in the MRR and SR due to the change in the selected EDM process parameters, along with SN ratios and mean, are reported in Table 4. To authenticate the results, all the experiments were repeated three times. Similarly, the output values (MRR and SR) of machined surfaces were measured three times, at different locations.

Table 4. Experimental results.

		Process Parameters			Response: MRR (mg/min)					Response: Ra (µm)				
Ex	Tool	I (A)	Ton (µs)	V (V)	MRR 1	MRR 2	MRR 3	SNRA	MEAN (+/−) 0.99	Ra 1	Ra 2	Ra 3	SNRA	MEAN (+/−) 0.2
1	Cu	10	120	4	59.56	58.82	60.29	35.497	59.557	4.6	4.7	4.5	−13.257	4.6
2	Cu	10	200	8	62.5	61.76	63.6	35.932	62.62	5.3	5.4	5.1	−14.433	5.2666
3	Cu	10	300	12	66.54	67.28	65.44	36.444	66.42	6	5.8	6.2	−15.566	6
4	Cu	12	120	4	77.94	78.68	77.21	37.834	77.943	5.1	4.9	5.3	−14.156	5.1
5	Cu	12	200	8	81.25	81.99	80.88	38.209	81.373	5.8	5.9	5.6	−15.221	5.7666
6	Cu	12	300	12	84.93	84.19	86.4	38.604	85.173	6.5	6.4	6.7	−16.304	6.5333
7	Cu	14	120	8	86.76	86.4	86.03	38.729	86.397	5.9	6	5.8	−15.418	5.9
8	Cu	14	200	12	90.07	90.44	89.34	39.079	89.95	6.6	6.4	6.8	−16.394	6.6
9	Cu	14	300	4	121.69	120.96	122.43	41.705	121.69	6.5	6.6	6.3	−16.215	6.4666
10	Br	10	120	12	37.87	37.13	38.6	31.561	37.867	4.9	4.8	5.1	−13.866	4.9333
11	Br	10	200	4	64.34	63.6	64.71	36.152	64.217	4.7	4.9	4.5	−13.447	4.7
12	Br	10	300	8	68.75	67.65	69.49	36.728	68.63	5.4	5.2	5.6	−14.652	5.4
13	Br	12	120	8	61.4	62.13	60.29	35.743	61.273	5.1	5.3	4.9	−14.156	5.1
14	Br	12	200	12	65.07	64.34	65.44	36.250	64.95	5.8	5.9	5.6	−15.221	5.7666
15	Br	12	300	4	97.06	97.43	96.32	39.729	96.937	5.6	5.5	5.8	−15.017	5.6333
16	Br	14	120	12	73.16	72.79	73.9	37.299	73.283	5.9	5.7	6.1	−15.42	5.9
17	Br	14	200	4	101.47	101.1	100.37	40.084	100.98	5.7	5.8	5.5	−15.069	5.6666
18	Br	14	300	8	105.51	104.78	105.88	40.455	105.39	6.4	6.5	6.3	−16.124	6.4

3.1. Influence on the Material Removal Rate (MRR)

The main effects plot for the mean MRR is shown in Figure 4. From Table 4 and Figure 4, it is clear that all the selected EDM parameters have a considerable effect on the MRR. Here, the analysis of variance (ANOVA) was used to analyze the results of the MRR based on higher-is-better criteria, as shown in Table 5. It is clear that the MRR increased with the rise in the current and the pulse duration. At a high discharge current, the higher MRR may be due to the high spark energy. The relatively high electrical conductivity in the copper electrode resulted in a higher MRR. In the fabricated Al6061/SiC/Gr composite, the addition of SiC and Gr particles increased the conductivity of the workpiece, resulting in a high MRR. On the other hand, the voltage did not turn out to be a significant EDM parameter in terms of its influence on the MRR. Figure 4 and Table 5 show the percentage contribution of each selected EDM parameter to the MRR. It can be observed that the current made a 58% contribution, followed by pulse duration: 27%; voltage: 13%; and tool material: 3%. A rank was assigned to various process parameters for MRR, on the basis of delta value, as shown in Table 6. Further, Figure 5 represents the surface morphology of machined workpieces. Figure 5a,b show the morphology of the material removal rate of a machined surface, and the melting and resolidification of the molten workpiece, respectively. The maximum material removal rate was measured in trial nine, and the reason for the high MRR was the generation of Lorentz forces via the interplay of electrical current, which enhanced the plasma pressure.

Table 5. Analysis of variance (ANOVA) for MRR.

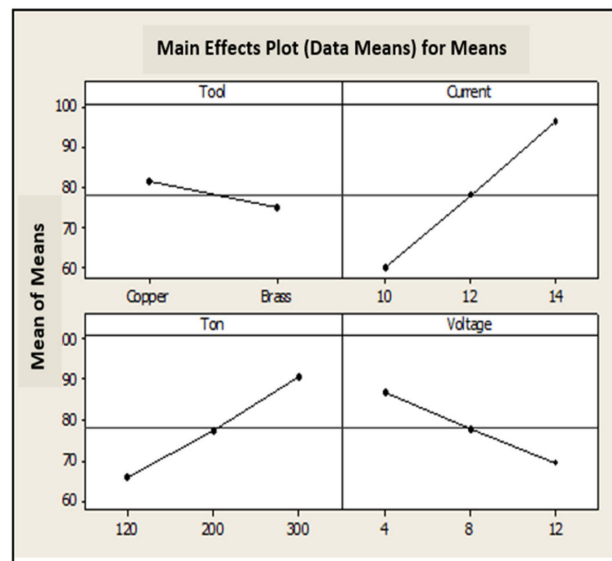| Source	DF	Seq SS	Adj SS	Adj MS	F	P	%C
Tool	1	184.32	184.32	184.32	186.67	0	2.67
Current (Amp)	2	3974.35	3974.3	1987.18	2012.5	0	57.65
T$_{on}$ (µs)	2	1827.7	1827.7	913.85	925.5	0	26.51
Voltage (V)	2	897.46	897.46	448.73	454.45	0	13.02
Residual error	10	9.87	9.87	0.99			0.14
Total	17	6893.71					100

Figure 4. Main effects plots (means) for MRR (mg/min) (units: current (Amp), voltage (V), T_{on} (µs)).
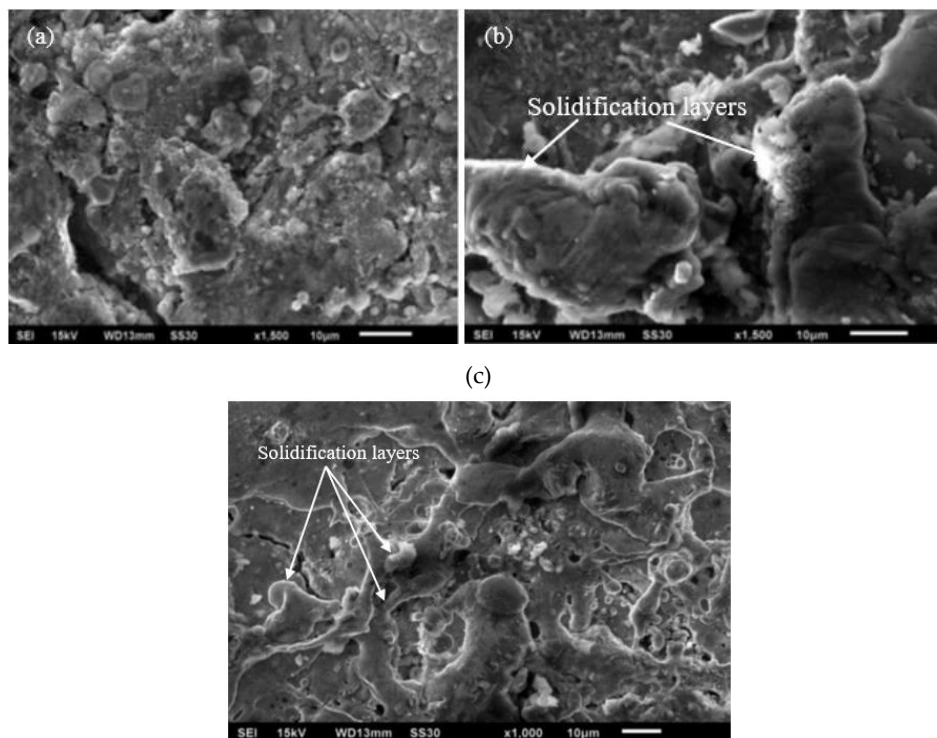

Figure 5. Scanning electron microscope (SEM) analysis of workpieces after machining (**a**,**b**): Al-12%, (**c**) Al-18%. (Note: EDM parameters for both (**a**) I = 10 (Amp), V= 4 (V), T_{on} = 200 (µs) and copper electrode, and (**b**,**c**) I = 14 (Amp), V= 4 (V), T_{on} = 200 (µs) and copper electrode.)

For the sake of this discussion, we compared the results of this study with those from our recent research [34]. The workpiece of this study, with 12% SiC particles, resulted in a high MRR and a comparatively high amount (18%) of SiC [34]. This is because the workpiece having a smaller amount of SiC increased its conductivity. The surface morphology of workpiece Al-Sic (18%) after the electrical discharge treatment is also represented in Figure 5c; it indicates the high melting and resolidification of the molten workpiece. The high SiC in the composite material exhibited a shielding effect and decreased the MRR.

Table 6. Response table for MRR (mg/min).

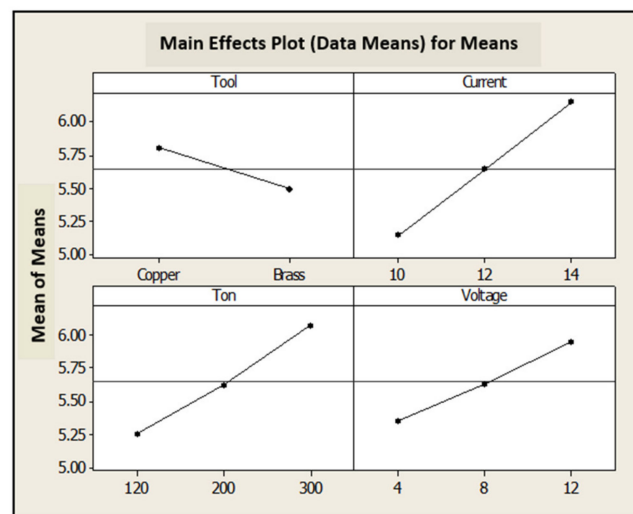| Level	Tool	Current (Amp)	Ton (μs)	Voltage (V)
1	81.24	59.89	66.05	86.89
2	74.84	77.94	77.35	77.61
3		96.28	90.71	69.61
Delta	6.4	36.4	24.65	17.28
Rank	4	1	2	3

3.2. Influence on the Surface Roughness (SR)

Surface roughness, often known as average surface roughness (R_a), is a component of surface texture. The surface roughness analysis of the machined surface described a true mark of the EDM electrode while machining and the material removal mechanism. The changes in SR due to changes in the selected EDM process parameters are reported in Table 7. The purpose of ANOVA (Table 7) was to investigate which of the process parameters significantly affect this performance characteristic, based on smaller-is-better criteria. The surface roughness measurements were carried out at different points of the machined surface. Further, from Table 7, it can clearly be seen that the machining parameters, such as current, voltage, and pulse duration, had a considerable effect on SR values. It is clear from the graph (Figure 6) that the brass electrode was also a significant factor affecting the surface roughness. Table 8 shows the percentage contribution of each selected EDM parameter to the SR. Here, in the case of surface roughness, the current contributed 47%, followed by pulse duration: 31%; voltage: 16%; and tool material: 6%. The ranks were assigned to the process parameters on the basis of delta value. The high current was responsible for distributing more heat to the workpiece surfaces, which consequently produced craters, and these craters caused the high surface roughness in the machined surfaces. The pulse-on time (T_{on}) was another significant factor that affected SR. An increase in the pulse-on time led to an increase in the machining duration, which resulted in an increase in the spark energy and radius of the plasma channel, which further increased the SR.

Trials one and eleven in Table 4 show that a smoother machined surface can only be achieved when EDM is carried out with a low current, voltage, and pulse duration. The Lorentz forces that developed while machining for a shorter duration made the machining zone smoother and decreased the roughness. From the SEM analysis shown in Figure 7, it can be observed that a significantly smoother surface occurred when current, voltage, and pulse duration were low. It is also observed that the SR was lower in the case of brass as compared to copper, because brass has a low ability to withstand spark energy. Therefore, it can be seen that thermal conductivity and the melting point of electrodes influence the output surface quality.

Table 7. Analysis of variance (ANOVA) for SR (R_a).

| Source	DF	Seq SS	Adj SS	Adj MS	F	P	%C
Tool	1	0.41506	0.41506	0.41506	960.57	0	6.37
Current (Amp)	2	3.03346	3.03346	1.51673	3510.14	0	46.52
Ton (μs)	2	2.00605	2.00605	1.00302	2321.29	0	30.77
Voltage (V)	2	1.0616	1.0616	0.5308	1228.43	0	16.28
Residual error	10	0.00432	0.0043	0.00043			0.07
Total	17	6.52049					100

Figure 6. Main effects plots (means) for SR (μm). (units: current (Amp), voltage (V), T_{on} (μs).)

Table 8. Response table for SR (μm).

Level	Tool	Current (Amp)	Ton (μs)	Voltage (V)
1	5.804	5.15	5.256	5.361
2	5.5	5.65	5.628	5.639
3		6.156	6.072	5.956
Delta	0.304	1.006	0.817	0.594
Rank	4	1	2	3
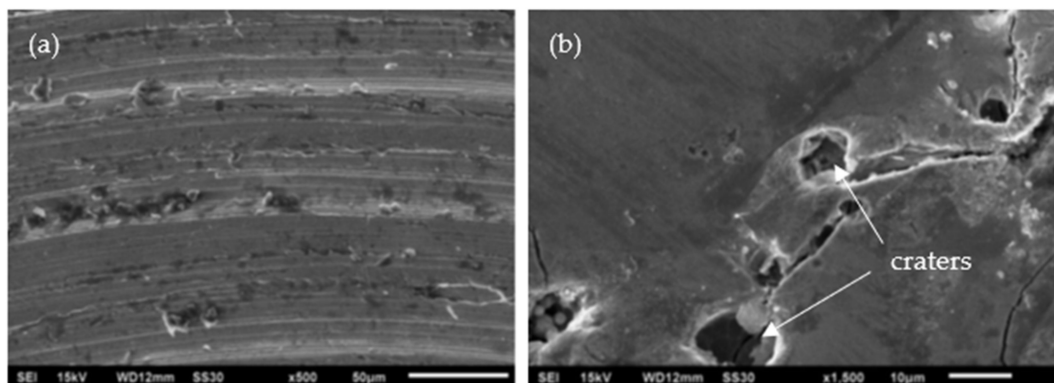
Figure 7. SEM images of machined workpieces: (**a**) R_a = 4.7 (μm) at I = 10 (Amp), V= 4 (V), Ton = 200 (μs) and brass electrode; (**b**) R_a = 5.4 (μm) at I = 10 (Amp), V= 4 (V), Ton = 200 (μs) and copper electrode.

3.3. Confirmation Experiments

In order to validate the regression equations, experimental data were compared with the data obtained via the same experimental conditions in the regression equations. The results for MRR and SR are tabulated in Tables 9 and 10, respectively. The results show that the experimental data and the data obtained from the regression equations closely correlate with each other, thus validating the regression equations developed.

Table 9. Confirmation test for MRR.

Process Parameters	Parameter Value	Experimental Value	Model Value	Variation
Tool Material	Copper			
Current (Amp)	14			
Pulse Duration (μs)	300	121.693	121.00	0.57%
Voltage (V)	4			

Table 10. Confirmation test for SR.

Process Parameters	Parameter Value	Experimental Value	Model Value	Variation
Tool Material	Brass			
Current (Amp)	10			
Pulse Duration (μs)	200	4.64	4.94	0.36%
Voltage (V)	4			

4. Conclusions

The newly developed hybrid metal matrix composite (Al6061/SiC/Gr) has superior mechanical properties when compared with a traditional metal matrix composite (Al6061/SiC) and pure Al6061. This research represents an experimental investigation of electric discharge machining as regards the newly developed Al6061/SiC/Gr hybrid metal matrix composite, which is fabricated via the stir casting process. To verify the contribution of each selected electrical discharge machining parameter (peak current, voltage, pulse-on time, and tool material), a statistical technique was used. Based on the observed results, the following conclusions can be drawn:

1. It was found that the addition of Gr and SiC particles led to superior mechanical and wear properties of a composite material. The hardness of Al6061/SiC/Gr rapidly increased by 40% compared to the base Al6061 hardness value.
2. The material removal rate of the new aluminum metal matrix composite increases from 50% to 60% with the rise in current and pulse duration, while it decreases by 20% with an increase in voltage. Moreover, in comparison to brass, a copper electrode is better-suited to achieving a high material removal rate in the newly developed Al6061/SiC(12%)/Gr(5%) composite.
3. The surface roughness of the new aluminum metal matrix composite (Al6061/SiC(12%)/ Gr(5%)) increases with an upsurge in the current, voltage and pulse duration, and brass is the best electrode to achieve low surface roughness (Ra).

Future scope: Prominent process parameters such as T_{off} and a magnetic field were not considered in this study. Though the electric discharge machining process parameters were thoroughly investigated for the aluminum matrix composite, there is still scope for further investigation into other hybrid aluminum metal matrix composites. In addition, the effect of other electric discharge machining process parameters that have not been included in this study, such as the type of dielectric, concentration of slurry, and tool geometry, may also be investigated.

Author Contributions: Conceptualization, data curation, formal analysis, methodology, writing—original draft, writing—review and editing, M.S. and H.K.G.; data curation, writing—review and editing, H.K.G., A.Y., S.M., R.S. and S.Y.; data curation, formal analysis, H.K.G., S.M., P.M., T.V.T.N., M.K.L. and S.Y. All authors have read and agreed to the published version of the manuscript.

References

1. Sharma, P.; Sharma, S.; Khanduja, D. A study on microstructure of aluminium matrix composites. *J. Asian Ceram. Soc.* **2015**, *3*, 240–244. [CrossRef]
2. Bodunrin, M.; Alaneme, K.; Chown, L. Aluminium matrix hybrid composites: A review of reinforcement philosophies, mechanical, corrosion and tribological characteristics. *J. Mater. Res. Technol.* **2015**, *4*, 434–445. [CrossRef]
3. Pandi, G.; Muthusamy, S. A review on machining and Tribological behaviors of aluminium hybrid Composites. *Procedia Eng.* **2012**, *38*, 1399–1408. [CrossRef]
4. Singh, G.; Sidhu, S.S.; Bains, P.S.; Singh, M.; Bhui, A.S. On surface Modification of Ti Alloy by Electro Discharge Coating Using Hydroxyapatite Powder Mixed Dielectric with Graphite Tool. *J. Bio-Tribo-Corros.* **2020**, *6*, 1–11. [CrossRef]
5. Zhu, Z.; Guo, D.; Xu, J.; Lin, J.; Lei, J.; Xu, B.; Wu, X.; Wang, X. Processing Characteristics of Micro Electrical Discharge Machining for Surface Modification of TiNi Shape Memory Alloys Using a TiC Powder Dielectric. *Micromachines* **2020**, *11*, 1018. [CrossRef] [PubMed]
6. Rengasamy, N.; Rajkumar, M.; Senthil Kumaran, S. An analysis of mechanical properties and optimization of EDM process parameters of Al 4032 alloy reinforced with Zrb_2 and Tib_2 in-situ composites. *J. Alloy. Compd.* **2016**, *662*, 325–338. [CrossRef]
7. Alaneme, K.; Sanusi, K. Microstructural characteristics, mechanical and wear behaviour of aluminium matrix hybrid composites reinforced with alumina, rice husk ash and graphite. *Eng. Sci. Technol. Int. J.* **2015**, *18*, 416–422. [CrossRef]
8. Singh, J.; Chauhan, A. Characterization of hybrid aluminum matrix composites for advanced applications–A review. *J. Mater. Res. Technol.* **2016**, *5*, 159–169. [CrossRef]
9. Radhika, N.; Subramanian, R.; Prasat, S. Tribological Behaviour of Aluminium/Alumina/Graphite Hybrid Metal Matrix Composite Using Taguchi's Techniques. *J. Miner. Mater. Charact. Eng.* **2011**, *10*, 427–443. [CrossRef]
10. Mahdavi, S.; Akhlaghi, F. Effect of SiC content on the processing, compaction behavior, and properties of Al6061/SiC/Gr hybrid composites. *J. Mater. Sci.* **2010**, *46*, 1502–1511. [CrossRef]
11. Shaikh, M.B.N.; Arif, S.; Siddiqui, M.A. Fabrication and characterization of aluminium hybrid composites reinforced with fly ash and silicon carbide through powder metallurgy. *Mater. Res. Express* **2018**, *5*, 46506. [CrossRef]
12. Arif, S.; Alam, M.T.; Ansari, A.H.; Shaikh, M.B.N.; Siddiqui, M.A. Analysis of tribological behaviour of zirconia reinforced Al-SiC hybrid composites using statistical and artificial neural network technique. *Mater. Res. Express* **2018**, *5*, 56506. [CrossRef]
13. Singh, M.; Mishra, P.K.; Mohaty, P.P.; Singh, R. Experimental Investigation of Tool Wear Rate (TWR) During the EDM of Hybrid Aluminum Metal Matrix Composite Reinforced with SiCp and Grp. In *Advances in Materials Processing and Manufacturing Applications*; Patnaik, A., Kozeschnik, E., Kukshal, V., Eds.; Lecture Notes in Mechanical Engineering; Springer: Singapore, 2021; pp. 409–419.
14. Sharma, S.; Singh, M.; Jayaram-Babu, N.; Rao, K.V.; Singh, J. Investigation of Properties of Mg and Al Based Nano Hybrid-Metallic Composites Processed Through Liquid Processing Technique. In *Advances in Design, Simulation and Manufacturing II.*; Ivanov, V., Ed.; Lecture Notes in Mechanical Engineering; Springer: Cham, Switzerland, 2019; pp. 466–476.
15. Singh, P.; Raghukandan, K.; Pai, B. Optimization by Grey relational analysis of EDM parameters on machining Al–10% SiCP composites. *J. Mater. Process. Technol.* **2004**, *155–156*, 1658–1661. [CrossRef]
16. Vishwakarma, U.K.; Dvivedi, A.; Kumar, P. FEA modeling of material removal rate in electrical discharge machining of Al6063/SiC composites. *Int. J. Mech. Aerosp. Eng.* **2012**, *6*, 398–403.
17. Bains, P.S.; Sidhu, S.S.; Payal, H.S.; Kaur, S. Magnetic Field Influence on Surface Modifications in Powder Mixed EDM. *Silicon* **2019**, *11*, 415–423. [CrossRef]
18. Akkurt, A. The effect of cutting process on surface microstructure and hardness of pure and Al 6061 aluminium alloy. *Eng. Sci. Technol. Int. J.* **2015**, *18*, 303–308. [CrossRef]
19. Barenji, R.; Pourasl, H.; Khojastehnezhad, V. Electrical discharge machining of the AISI D6 tool steel: Prediction and modeling of the material removal rate and tool wear ratio. *Precis. Eng.* **2016**, *45*, 435–444. [CrossRef]
20. Liu, Q.Y.; Zhang, Q.H.; Zhang, M.; Yang, F.Z. Study on the discharge characteristics of single-pulse discharge in Micro-EDM. *Micromachines* **2020**, *11*, 55. [CrossRef] [PubMed]
21. Bilal, A.; Jahan, M.P.; Talamona, D.; Perveen, A. Electro-discharge machining of ceramics: A review. *Micromachines* **2019**, *10*, 10. [CrossRef] [PubMed]
22. Wyszynski, D.; Bizon, W.; Miernik, K. Electrodischarge drilling of microholes in c-BN. *Micromachines* **2020**, *10*, 179. [CrossRef]
23. Das, M.; Kumar, K.; Barman, T.; Sahoo, P. Optimization of Surface Roughness and MRR in EDM Using WPCA. *Procedia Eng.* **2013**, *64*, 446–455. [CrossRef]

24. Roy, T.; Balasubramaniam, R. Influence of ion-rich plasma discharge channel on unusually high discharging points in reverse micro electrical discharge machining. *Int. J. Adv. Manuf. Technol.* **2020**, *106*, 4467–4475. [CrossRef]
25. George, P.; Raghunath, B.; Manocha, L.; Warrier, A. EDM machining of carbon–carbon composite—A Taguchi approach. *J. Mater. Process. Technol.* **2004**, *145*, 66–71. [CrossRef]
26. Maniraj, S.; Thanigaivelan, R.; Viswanathan, R.; Elumalai, P. Experimental investigation of MRR and ROC in aluminium metal matrix composites. *Mater. Today Proc.* **2021**, *45*, 1102–1106.
27. Malhotra, P.; Tyagi, R.K.; Singh, N.K.; Sikarwar, B.S. Experimental investigation and effects of process parameters on EDM of Al7075/SiC composite reinforced with magnesium particles. *Mater. Today Proc.* **2020**, *21*, 1496–1501. [CrossRef]
28. Lakshmanan, P.; Kumanan, G.; Arunkumar, L.; Amith, S.C. Experimental investigations of material removal rate on Mg/SiCp-flyash hybrid metal matrix composites by electrical discharge machining. *Mater. Today Proc.* **2021**, *46*, 986–990.
29. Kannan, A.; Mohan, R.; Viswanathan, R.; Sivashankar, N. Experimental investigation on surface roughness, tool wear and cutting force in turning of hybrid (Al7075 + SiC + Gr) metal matrix composites. *J. Mater. Res. Technol.* **2020**, *9*, 16529–16540. [CrossRef]
30. Ablyaz, T.R.; Bains, P.S.; Sidhu, S.S.; Muratov, K.R.; Shlykov, E.S. Impact of Magnetic Field Environment on the EDM Performance of Al-SiC Metal Matrix Composite. *Micromachines* **2021**, *12*, 469. [CrossRef]
31. James, S.; Venkatesan, K.; Kuppan, P.; Ramanujam, R. Hybrid Aluminium Metal Matrix Composite Reinforced with SiC and TiB2. *Procedia Eng.* **2014**, *97*, 1018–1026. [CrossRef]
32. Suresh, S.; Moorthi, N. Process Development in Stir Casting and Investigation on Microstructures and Wear Behavior of TiB$_2$ on Al6061 MMC. *Procedia Eng.* **2013**, *64*, 1183–1190. [CrossRef]
33. Bhandare, R.G.; Sonawane, P.M. Preparation of aluminium matrix composite by using stir casting method. *Int. J. Eng. Adv. Technol.* **2013**, *3*, 61–65.
34. Singh, M.; Maharana, S. Investigating the EDM parameter effects on aluminium based metal matrix composite for high MRR. *Mater. Today Proc.* **2020**, *33*, 3858–3863. [CrossRef]
35. Weng, W.C.; Choi, T.M. Optimization Comparison between Taguchi's Method and PSO by Design of a CPW Slot Antenna. In Proceedings of the IEEE Antennas and Propagation Society International Symposium, Seattle, WA, USA, 20–24 June 2009; pp. 1–4.
36. Bahgat, M.M.; Shash, A.Y.; Abd-Rabou, M.; El-Mahallawi, I.S. Influence of process parameters in electrical discharge machining on H13 die steel. *Heliyon* **2019**, *5*, e01813. [CrossRef] [PubMed]